Ferenc Toth   ORCID iD: 0000-0002-6615-389X

Kai Ludwig   ORCID iD: 0000-0001-9867-9346

Evaluation of the Suitability of Miniature Pigs as an Animal Model of Juvenile Osteochondritis Dissecans

Authors: Ferenc Tóth[1] DVM, Ph.D, Casey P. Johnson[2] Ph.D, Benigno Mills, Mikko J.

Nissi[3,4] Ph.D, Olli Nykänen[3] M.Sc, Jutta Ellermann[2] MD, Ph.D, Kai D. Ludwig[2] Ph.D.,

Marc Tompkins[5] MD, Cathy S. Carlson[6] DVM, Ph.D

Affiliations:

[1]Department of Veterinary Population Medicine, University of Minnesota, St. Paul, MN

[2]Center for Magnetic Resonance Research, Department of Radiology, University of

Minnesota, Minneapolis, MN

[3]Department of Applied Physics, University of Eastern Finland, Kuopio, Finland

[4]Research Unit of Medical Imaging, Physics and Technology, University of Oulu, Oulu,

Finland

[5]Department of Orthopedic Surgery, University of Minnesota, Minneapolis, MN

[6]Department of Veterinary Clinical Sciences, University of Minnesota, St. Paul, MN

*Address correspondence to: Ferenc Tóth, 295R AnSci/VetMed, CVM, 1365 Gortner

Avenue, St. Paul, MN 55108, USA; Tel.: 1-612-624-7727; ftoth@umn.edu

Running title: Miniature pig model of JOCD

Author contribution: All authors have substantially contributed to various parts of collection, analysis, and interpretation of data and have critically reviewed and approved the submitted and final versions of the manuscript.

Abstract:

Juvenile osteochondritis dissecans (JOCD) is a developmental disease characterized by formation of intra-articular (osteo)chondral flaps or fragments. Evidence-based treatment guidelines for JOCD are currently lacking. An animal model would facilitate study of JOCD and evaluation of diagnostic and treatment approaches. The purpose of this study was to assess the suitability of miniature pigs as a model of JOCD at the distal femur. First, stifle (knee) joints harvested from three juvenile miniature pigs underwent MRI to establish the vascular architecture of the distal femoral epiphyseal cartilage. Second, vessels supplying the axial or abaxial aspects of the medial femoral condyle were surgically interrupted in four additional juvenile miniature pigs, and the developing epiphyseal cartilage lesions were monitored using three consecutive MRI examinations over nine weeks. The miniature pigs were then euthanized, and their distal femora were harvested for histological evaluation. Vascular architecture of the distal femoral epiphyseal cartilage in the miniature pigs was found to be nearly identical to that of juvenile human subjects, characterized by separate vascular beds supplying the axial and abaxial aspects of the condyles. Surgical interruption of the vascular supply to the abaxial

aspect of the medial femoral condyle resulted in ischemic cartilage necrosis (a precursor lesion of JOCD) in 75% (3/4) of the miniature pigs. Cartilage lesions were identified during the first MRI performed 3 weeks post-operatively. No clinically-apparent JOCD-like lesions developed. In conclusion, miniature pigs are suitable for modelling JOCD precursor lesions. Further investigation of the model is warranted to assess induction of clinically-apparent JOCD lesions.

Keywords: Miniature pig, JOCD, osteochondrosis, knee, animal model

Introduction

Juvenile osteochondritis dissecans (JOCD) is an orthopaedic disease characterized by intra-articular formation of osteo-cartilaginous flaps and fragments in pediatric and adolescent patients[1]. Nearly 62% of all JOCD lesions involve the distal femur, with the ankle, elbow and shoulder joints affected at decreasing frequencies[2]. To delay progression toward early onset osteoarthritis, clinically-apparent JOCD lesions are treated using either conservative or surgical techniques[1]. Unfortunately, evidence-based treatment guidelines for JOCD are lacking[3] because the low incidence of the disease limits the opportunity to conduct large-scale studies. Animal models represent an alternative approach to provide data that are critically needed to inform clinical decision making.

The pathogenesis of JOCD in human patients is incompletely understood. Multiple theories are proposed to describe its development, including inadequate vascular supply to the subchondral bone, repeated trauma, and genetic factors[4-7]. However, results of recent studies strongly suggest that failure of the vascular supply to the epiphyseal

growth cartilage (i.e., immature joint cartilage located beneath the articular cartilage at the ends of growing long bones) plays a central role in the development of JOCD[8-10]. These findings are not unexpected considering that vascular failure is known to be the inciting factor for osteochondrosis (OC), a naturally-occurring disease of animals that is nearly identical in its presentation to JOCD[7; 11]. In multiple animal species, the pathogenesis of OC has been shown to begin with a failure of the vascular supply to the epiphyseal growth cartilage that results in formation of discrete areas of epiphyseal cartilage necrosis. This earliest subclinical stage of the disease involves neither the overlying articular cartilage nor the subchondral bone and is termed *OC latens*. In areas of epiphyseal cartilage necrosis, physiologic replacement of epiphyseal growth cartilage with bone is delayed, causing a failure of enchondral ossification, a stage of the disease that is termed *OC manifesta*[11]. The clinically-apparent disease, *osteochondrosis dissecans* (OCD), is thought to develop because the necrotic epiphyseal cartilage is unable to support the overlying articular cartilage during repeated exposure to biomechanical forces, which leads to the formation of osteochondral fragments and/or cleft(s) extending through cartilage[7]. In animals, these clefts often involve the articular cartilage. Although the dissecans stage (presence of flaps/fragments) of the disease has long been recognized in humans, *OC latens* and *OC manifesta* have only recently been documented in human subjects[8-10]. Because humans have a much slower rate of maturation than animals (years vs. months), and because surgical intervention in humans typically occurs much later after initial diagnosis than in animals (months to years vs. days to weeks), chronic stages of the disease in humans are commonly characterized by mineralization of the necrotic epiphyseal cartilage with varying degrees of osseous bridging with the parent bone[8].

Involvement of the articular cartilage, both in humans and animals, invariably predisposes the joint to premature osteoarthritis[4].

Based on the increasingly accepted role that vascular compromise plays in the development of OCD and JOCD, it is imperative that animal models intended for recapitulating the human disease (JOCD) have similar vascular architecture to that seen in humans. Furthermore, disease induction in the prospective animal model should involve manipulation of the epiphyseal vascular supply[12]. These requirements are illustrated by results of previous studies that attempted to use goats to model JOCD and were only successful in inducing subclinical disease[13; 14]. In these studies, most of the induced *OC latens* and *OC manifesta* lesions exhibited signs of repair rather than developing into clinically apparent disease. Rich, collateral vascular supply to the distal femoral epiphyseal cartilage present in goats, but absent in humans, likely mediated this enhanced healing process.

In the study reported here, we evaluated the suitability of miniature pigs to serve as animal models of JOCD. The primary objectives of our study were to: 1) compare the vascular supply to the distal femoral epiphyseal cartilage in juvenile miniature pigs to that described in young human subjects; and 2) evaluate the effects of surgical interruption of the axial ('central' or 'intercondylar notch' side) or abaxial (peripheral) vascular beds supplying the medial femoral condylar epiphyseal cartilage in miniature pigs. We hypothesized, based on previous work in domestic pigs, that the vascular supply to the distal femoral epiphyseal cartilage in miniature pigs included an axial and an abaxial vascular bed in both the medial and lateral femoral condyles, identical to that demonstrated in human subjects[12]. We also hypothesized that surgical disruption of either

of these vascular beds would result in ischemic necrosis of the portion of the medial femoral condylar epiphyseal cartilage supplied by the affected vessels, followed by the development of *OC latens*, *OC manifesta* and *OC dissecans* lesions.

Materials and methods

Experimental design – The study was approved by the University of Minnesota Institutional Animal Care and Use Committee and was conducted in two stages. In the first stage, n = 3 cadaveric, unilateral stifle joint specimens obtained from Sinclair miniature pigs underwent *ex vivo* high-resolution MRI to allow detailed visualization of the epiphyseal vascular architecture[15]. In the second stage of the study, n = 4 Sinclair miniature pigs received bilateral stifle joint surgery to interrupt the vascular supply to the axial ('central' or 'intercondylar notch' side) aspect of the medial femoral condyle in the right pelvic limb and to the abaxial (peripheral) aspect of the medial femoral condyle in the left pelvic limb. Operated pigs underwent three consecutive *in vivo* MRI examinations to screen for the presence of *OC latens* and/or *OC manifesta* lesions. After the conclusion of the final MRI session, the miniature pigs were euthanized, and distal femoral specimens were collected for histological analysis.

Stage 1 – Visualization of the vascular architecture of the distal femoral epiphyseal cartilage:

Stifle joint specimens (n=3) obtained from three Sinclair miniature pigs aged 18, 33 and 48 days underwent *ex vivo* imaging using a preclinical 9.4T MRI scanner (Agilent Technologies; Santa Clara, CA) running VnmrJ software (version 4.2; Varian NMR Systems; Palo Alto, CA). A custom-built saddle transceiver coil was used for all

acquisitions. The specimens were immersed in perfluoropolyether (Fomblin; Specialty Fluids; Castaic, CA) to have a ^{1}H signal-free, susceptibility-matched background on the MR images. Imaging data were acquired using a 3D gradient recalled echo (GRE) sequence with an acquisition matrix of 384×384×384 and field-of-view of 38.4×38.4×38.4 mm^3, resulting in an isotropic resolution of 100 µm. Other acquisition parameters were: TE / TR = 15.3 / 40 ms, receiver bandwidth = 14 kHz (36.6 Hz/pixel) and flip angle = 15°. With these parameters, utilizing no undersampling or other accelerations, the scan time per specimen was 98 minutes[16].

Image processing – The 3D GRE datasets acquired at 9.4T MRI were processed for quantitative susceptibility mapping (QSM) to visualize the vascular structures in the cartilage canals using an approach similar to that previously described[15, 17-19]. The QSM processing consisted of first manually creating a mask for the articular-epiphyseal cartilage complex (AECC) using ITK-SNAP (www.itksnap.org). Subsequently, the field map was calculated from the phase data in the masked region utilizing Laplacian unwrapping (cutoff frequency = 10^{-10})[20] followed by variable-kernel sophisticated harmonic artifact reduction for phase data (V-SHARP) background field removal (the SHARP threshold was set to 0.5 and kernel radius varied between 2 and 9)[21]. The parameters of the V-SHARP were deliberately set to provide slightly more aggressive removal of the background fields than what an "optimal" setting would provide to improve the homogeneity of the background tissue and thus allow for clearer visualization of the vascular structures. Finally, the susceptibility map was calculated from the processed field map using morphology enabled dipole inversion (MEDI)[22]. The regularization parameter lambda in MEDI was set to 50,000 based on visual inspection of

results after experimenting with a wide range of lambdas. Finally, 3D volume rendering reconstructions were generated from the masked susceptibility maps using Osirix (Osirix v.8.0 64-bit, http://www.osirix-viewer.com/)[23].

Stage 2 – Surgical induction and monitoring of OC lesions:

Surgical interruption of the vascular supply to the distal femoral epiphyseal cartilage – Four male Sinclair miniature pigs aged 31 (n=2) and 34 (n=2) days weighing 1.8, 2.4, 3.9, 4.6 kg were enrolled in the study. Miniature pigs were sedated with an intramuscular (IM) administration of morphine (0.2 mg/kg) and midazolam (0.2 mg/kg. An intravenous catheter was placed into the auricular vein. Ceftiofur (2.2 mg/kg) was administered intravenously (IV) followed by induction of general anesthesia with IV administration of ketamine (5 mg/kg) and propofol (3 mg/kg). Anesthesia was maintained by inhalation of isoflurane vaporized in oxygen.

After routine surgical preparation and draping of both stifle (knee) joints, the right stifle joint was approached via a lateral parapatellar arthrotomy. The patella was luxated medially and the stifle joint was brought into complete flexion, exposing the trochlear ridges and the intercondylar groove. The infrapatellar fat pad was partially excised and a 5×5 mm^2 area of perichondrium along with a 1-mm-wide portion of the underlying AECC and subchondral bone was resected from the extreme axial, cranialmost (anteriormost) aspect of the medial femoral condyle adjacent to the intercondylar groove using a #15 scalpel blade. The left stifle was approached using an identical technique, but this time the 5×5 mm^2 area of perichondrium along with a 1-mm-wide portion of the underlying AECC and subchondral bone was resected from the abaxial aspect of the

cranio-caudal (anterio-posterior) midpoint of the medial femoral condyle. Upon completion of the procedure, the joint capsule along with the overlying muscles was closed using 3-0 PDS in a simple continuous pattern. Apposition of the subcutaneous tissues was also done using 3-0 PDS in a simple continuous pattern. Skin closure was completed using 3-0 Monocryl using an intradermal pattern. A sterile bandage covering the incision was applied to both limbs before the miniature pigs were allowed to recover.

Post-operatively, miniature pigs were housed together and were administered 1.1 mg/kg flunixin meglumine and 2.2 mg ceftiofur IM once daily for 3 days. No postoperative complications requiring additional veterinary interventions were encountered throughout the study period.

In vivo MRI of operated miniature pigs – In vivo MRI was conducted using a 3T MRI scanner (Signa HDxt; GE Healthcare; Waukesha, WI) with the miniature pigs anesthetized using an identical technique to that described for the surgical procedure. The miniature pigs were imaged at three consecutive time points (~3, ~4, and ~9 weeks post-operatively) to assess progression of lesions in both stifles. The same imaging protocol was used in all cases, and the right and left stifles were imaged separately. For imaging, the miniature pigs were placed in dorsal recumbency and their stifles were positioned within a quadrature knee receiver coil at the isocenter of the MR scanner. Imaging sequences included: 2D proton-density-weighted, T1-weighted, and T2-weighted fast spin echo (FSE); 3D T2-weighted FSE; and 2D GRE with a short echo time (TE = 3.0 ms). Lesions, including areas of altered intensity involving the epiphyseal growth cartilage with or without associated delay of the enchondral ossification, observed on MRI were identified by an independent observer who was blinded to the surgery.

Histological evaluation – Immediately after completion of the third MRI session (~9 weeks post-surgery), anesthetized miniature pigs were euthanized by IV administration of KCl (1 mEq/kg) and their distal femora were harvested for histological evaluation. Harvested distal femoral specimens were fixed in 10% neutral buffered formalin for 48 hours and then decalcified by immersion in EDTA solution. Decalcified medial (operated) and lateral (control) femoral condyles were bread-sliced in the coronal plane creating four to five 5-mm-thick slabs. Individual slabs were routinely processed and paraffin embedded. A 5-μm thick section was obtained from the surface of each slab, stained with hematoxylin and eosin (H&E) and examined for the presence of epiphyseal cartilage necrosis and/or failure of endochondral ossification using light microscopy. Failure of endochondral ossification was defined as the presence of focally thickened cartilage accompanied by a focal delay in the progression of the ossification front at the chondro-osseous junction. Cartilage necrosis was defined as the combined presence of shrunken, necrotic chondrocytes (characterized by pyknotic nuclei) and altered staining (pallor), sometimes accompanied by cystic degeneration (an area where loss of tissue/matrix components results in clear spaces replacing the matrix), of the surrounding matrix[13; 14].

Results:

Vascular architecture – In all three specimens, *ex vivo* MRI demonstrated that the vascular supply to the distal femoral epiphyseal cartilage included two distinct vascular beds in each condyle, one supplying the abaxial and another supplying the axial portion of the condyle. Animal age did not appear to influence the appearance of the vascular

architecture, as vessels tended to originate from the perichondrium, formed no apparent anastomoses, and traversed the epiphyseal cartilage parallel with the articular surface, as shown in Figure 1. An avascular region, more pronounced in the medial (compared to the lateral) femoral condyle, separated the two vascular beds. This characteristic vascular architecture bears a stark resemblance to that identified in our previous study[12] in the distal femoral epiphyseal cartilage in human beings (Figure 1, supplementary files 1-4).

In vivo MRI – OC-like lesions were identified in the left medial femoral condyles in 3/4 miniature pigs, which received surgery to interrupt the vascular supply to the abaxial aspect of the condyle. Developing lesions were best identified in T2 weighted images. During the final MRI session performed at 63, 64, 66, and 69 days post-operatively for miniature pigs 1, 2, 3, and 4, respectively, an *OC latens* lesion (evidenced by a focal T2 hyperintensity present within the epiphyseal cartilage) was identified in miniature pig 2 (Figure 2) and *OC manifesta* lesions (evidenced by T2 hyperintensity in the epiphyseal cartilage and associated delay in the progression of the ossification front) were identified in miniature pigs 1 (Figure 3) and 3 (Figure 4). Conversely, beyond the presence of a surgical scar, no abnormalities were identified in any of the right medial femoral condyles that received surgery to interrupt the vascular supply to the axial aspect of the condyle.

In the fourth miniature pig, difficulties with surgical exposure of the left femoral condyle resulted in an excessively cranial placement of the incision intended to disrupt the vascular supply to the abaxial aspect of the medial condyle. Although no MRI changes affecting either femoral condyle were noted in this miniature pig, changes characterized by marked T2 hyperintensity were present in the distal aspect of the medial

trochlear ridge of the femur. Temporal progression of lesions identified by MRI are summarized in Table 1.

Histological evaluation – Well-demarcated areas of epiphyseal cartilage necrosis were identified in the abaxial aspect of the left medial femoral condyle in 3 out of 4 miniature pigs (pigs 1, 2, and 3). Areas of cartilage necrosis contained degenerative cartilage canal vessels and were characterized by the presence of chondrocytes with pyknotic nuclei and marked pallor of the extracellular matrix (Figures 2, 3, and 4). The presence of necrotic epiphyseal cartilage caused a failure of enchondral ossification (i.e., delayed replacement of epiphyseal cartilage with bone) in 2 out of 4 left medial femoral condyles (Pigs 1 and 3). Conversely, surgical interruption of the vascular supply to the axial aspect of the right medial femoral condyle was unsuccessful as demonstrated by the presence of patent cartilage canals and lack of epiphyseal cartilage necrosis in all four miniature pigs.

Discussion:

Our results establish the feasibility of using miniature pigs as animal models of preclinical JOCD. Nearly identical vascular architecture of the developing femoral condyles between juvenile human subjects and miniature pigs was demonstrated, and lesions consistent with subclinical osteochondrosis were induced by interruption of the vascular supply to the abaxial aspect of the medial femoral condyle in three out of four miniature pigs.

Anatomical studies describing the vascular architecture of the epiphyseal cartilage at OC predilection sites in animal species[24-27] were first prompted by the discovery of the

role vascular failure plays in the development of OC.[28-31] Findings from these animal studies motivated subsequent experiments on cadaveric specimens obtained from juvenile human subjects that characterized the vascular architecture of epiphyseal cartilage of the distal femur, the primary predilection site of JOCD[12; 15]. These anatomical studies identified a characteristic vascular pattern present at predilection sites of OC/JOCD in various species, including humans, and provided additional support to the hypothesis that OC is initiated when sparse, long epiphyseal vessels fail at the level of the advancing ossification front[32]. In the current study, we have successfully shown that, although the lack of published literature suggests that miniature pigs are free of naturally-occurring OC, their epiphyseal vascular architecture closely resembles that seen in human subjects[12; 15] and domestic swine[27]. Specifically, in all three examined miniature pigs, separate vascular beds supplying the axial and abaxial aspects of the distal femoral condyles were identified along with epiphyseal cartilage vessels arising from the perichondrium that were oriented parallel with the articular surface of the femoral condyles and trochlea. Interestingly, the vascular architecture and density appeared qualitatively unchanged across the age range (18-34 days) of the miniature pigs that were examined. This is most likely explained by the overall young age of the three piglets studied, for which progressive replacement of the epiphyseal cartilage with bone was limited. It is also possible that the strictly qualitative nature of this observation did not allow detection of minute differences in vasculature among pigs of different ages. This finding suggests there is an urgency to develop quantitative imaging tools to better describe changes in vascular density and orientation in the epiphyseal cartilage.

In contrast to a previous study in goats, which aimed to create a lesion that is identical in its appearance to end-stage JOCD[33], in the current study we aimed to capture the purported pathogenesis of naturally-occurring JOCD in our proposed animal model[8; 11]. The surgeries resulted in epiphyseal cartilage necrosis (*OC latens* and/or *OC manifesta*) in three of four miniature pigs when the intervention involved the abaxial aspect of the medial condyle. Failure of sustained interruption of the vascular supply to the axial aspect of the medial femoral condyle interfered with induction of OC latens and/or OC manifesta lesions in this area. Visual analysis of the vascular supply to the axial versus abaxial aspect of the medial condyle did not identify any obvious differences that might explain this phenomenon. Therefore, establishing whether this failure stemmed from incomplete interruption of the vascular supply at the time of surgery or it was due to revascularization occurring in the post-operative period remains undetermined. In future studies, histological evaluation of the resected $5\times5\times1$ mm^3 osteochondral segments and/or the purported avascular portion of the epiphyseal cartilage in selected animals euthanized within 3 – 5 days after the surgical procedure represents an opportunity to establish whether successful interruption of the epiphyseal vascular supply is accomplished.

Induction of OC-like lesions by interruption of the vascular supply has been attempted previously. Initial 'proof-of-principle' experiments were conducted to confirm the role vascular failure plays in the pathogenesis of OC in domestic animals. Surgical interruption of the epiphyseal vascular supply led to the development of OC-like lesions in both domestic pigs[34; 35] and horses[36], unambiguously proving the role vascular failure plays in the development of OC. Importantly, these experiments did not aim to develop

an animal model of human JOCD, and were performed on animal species that are ill-suited to serve in translational studies. Both horses and domestic swine have a high incidence of naturally-occurring OC and their size and associated housing challenges make them poor choices for long-term studies[37; 38]. In our current study, we took a decidedly different route by carefully selecting a species that has a strong translational potential. Miniature pigs are well-established as animal models of various diseases, are not known to develop naturally-occurring OC, and their vascular architecture of the epiphyseal cartilage of the distal femur is similar to that of humans'.

Employing miniature pigs marks a transition from our previous studies that used goats in an attempt to develop a clinically-relevant animal model of JOCD [13; 14]. Goats were selected for these earlier studies based on their previous successful use as animal models of orthopaedic disease, small size to enable imaging in available MRI scanners, and relatively long lifespan, while initially no consideration was given to vascular anatomy. We found that epiphyseal cartilage lesions triggered by interruption of the vascular supply in the goats were limited in size and exhibited a low propensity to develop into clinically apparent OCD[13; 14]. Results of subsequent studies identified an extensive collateral vascular architecture composed of short, branching vessels in the caprine distal femoral epiphyseal cartilage that was markedly different from that seen in human subjects and domestic swine[12]. This difference in vascular architecture provides a highly plausible explanation why induced OC lesions are comparatively small and tend to heal in goats.

Limitations of the present study included a small sample size and the qualitative nature of our results. In future studies, it would be interesting to quantitate the age

dependent regression of the epiphyseal vascular supply of the distal femur in miniature

pigs and compare this process to changes described in other species, particularly humans.

It would also be valuable to study the progression of the surgically-induced lesions over a

longer duration. While we successfully induced *OC-latens* and *OC-manifesta* lesions in

the miniature pigs, the 9-week post-surgical timeframe proved insufficient to result in

clinically-apparent OCD lesions (i.e., fragmentation and/or cleft formation extending

through cartilage). Our inability to demonstrate clinically apparent OCD lesions in the

operated pigs may be explained by the insufficient size of the induced lesions or by

inadequate exposure to biomechanical force during the post-operative period.

Nevertheless, the presence of OCM lesions at the time of euthanasia suggests that these

subclinical lesions had the potential to progress to clinical disease. Thus, exposing the

operated piglets to biomechanical force, after the presence of *OC-manifesta* lesions are

confirmed by MRI, may promote progression of the lesions to clinical disease in future

studies. Alternatively, further investigation may be aimed at altering the surgical

procedure in order to induce lesions of larger volume.

In summary, miniature pigs have the potential to be highly relevant translational

animal models of JOCD. These animals have nearly identical vascular architecture in the

distal femoral condyles to humans, which is a primary predilection site for JOCD, and

interruption of these vessels results in the development of subclinical OC lesions.

References:

1.   Adachi N, Deie M, Nakamae A, et al. 2015. Functional and radiographic outcomes of unstable juvenile osteochondritis dissecans of the knee treated with lesion fixation using bioabsorbable pins. J Pediatr Orthop 35:82-88.

2.   Weiss JM, Nikizad H, Shea KG, et al. 2016. The Incidence of Surgery in Osteochondritis Dissecans in Children and Adolescents. Orthop J Sports Med 4:2325967116635515.

3.   Chambers HG, Shea KG, Anderson AF, et al. 2012. American Academy of Orthopaedic Surgeons clinical practice guideline on: the diagnosis and treatment of osteochondritis dissecans. J Bone Joint Surg Am 94:1322-1324.

4.   Cahill BR. 1995. Osteochondritis Dissecans of the Knee: Treatment of Juvenile and Adult Forms. J Am Acad Orthop Surg 3:237-247.

5.   Crawford DC, Safran MR. 2006. Osteochondritis dissecans of the knee. J Am Acad Orthop Surg 14:90-100.

6.   Edmonds EW, Polousky J. 2013. A review of knowledge in osteochondritis dissecans: 123 years of minimal evolution from Konig to the ROCK study group. Clin Orthop Relat Res 471:1118-1126.

7. McCoy AM, Toth F, Dolvik NI, et al. 2013. Articular osteochondrosis: a comparison of naturally-occurring human and animal disease. Osteoarthritis Cartilage 21:1638-1647.

8. Ellermann J, Johnson CP, Wang L, et al. 2017. Insights into the Epiphyseal Cartilage Origin and Subsequent Osseous Manifestation of Juvenile Osteochondritis Dissecans with a Modified Clinical MR Imaging Protocol: A Pilot Study. Radiology 282:798-806.

9. Tóth F, Tompkins MA, Shea KG, et al. 2018. Identification of Areas of Epiphyseal Cartilage Necrosis at Predilection Sites of Juvenile Osteochondritis Dissecans in Pediatric Cadavers. J Bone Joint Surg Am 100:2132-2139.

10. Olstad K, Shea KG, Cannamela PC, et al. 2018. Juvenile osteochondritis dissecans of the knee is a result of failure of the blood supply to growth cartilage and osteochondrosis. Osteoarthritis Cartilage 26:1691-1698.

11. Olstad K, Ekman S, Carlson CS. 2015. An Update on the Pathogenesis of Osteochondrosis. Vet Pathol 52:785-802.

12. Toth F, Nissi MJ, Ellermann JM, et al. 2015. Novel Application of Magnetic Resonance Imaging Demonstrates Characteristic Differences in Vasculature at Predilection Sites of Osteochondritis Dissecans. Am J of Sports Med 43:2522-2527.

13.   Toth F, Nissi MJ, Wang L, et al. 2015. Surgical induction, histological evaluation, and MRI identification of cartilage necrosis in the distal femur in goats to model early lesions of osteochondrosis. Osteoarthritis Cartilage 23:300-307.

14.   Tóth F, David FH, LaFond E, et al. 2017. In vivo visualization using MRI T2 mapping of induced osteochondrosis and osteochondritis dissecans lesions in goats undergoing controlled exercise. J Orthop Res 35:868-875.

15.   Nissi MJ, Tóth F, Wang L, et al. 2015. Improved Visualization of Cartilage Canals Using Quantitative Susceptibility Mapping. PLoS One 10:e0132167.

16.   Nissi MJ, Toth F, Zhang J, et al. 2014. Susceptibility weighted imaging of cartilage canals in porcine epiphyseal growth cartilage ex vivo and in vivo. Magn Reson Med 71:2197-2205.

17.   Nykänen O, Rieppo L, Töyräs J, et al. 2018. Quantitative susceptibility mapping of articular cartilage: Ex vivo findings at multiple orientations and following different degradation treatments. Magn Reson Med 80:2702-2716.

18.   Wei H, Gibbs E, Zhao P, et al. 2017. Susceptibility tensor imaging and tractography of collagen fibrils in the articular cartilage. Magn Reson Med 78:1683-1690.

19.   Wang L, Nissi MJ, Toth F, et al. 2017. Quantitative susceptibility mapping detects abnormalities in cartilage canals in a goat model of preclinical osteochondritis dissecans. Magn Reson Med 77:1276-1283.

20. Schofield MA, Zhu Y. 2003. Fast phase unwrapping algorithm for interferometric applications. Optics Letters 28:3.

21. Wu B, Li W, Guidon A, et al. 2012. Whole brain susceptibility mapping using compressed sensing. Magn Reson Med 67:137-147.

22. de Rochefort L, Liu T, Kressler B, et al. 2010. Quantitative susceptibility map reconstruction from MR phase data using bayesian regularization: validation and application to brain imaging. Magn Reson Med 63:194-206.

23. Rosset A, Spadola L, Ratib O. 2004. OsiriX: an open-source software for navigating in multidimensional DICOM images. J Digit Imaging 17:205-216.

24. Olstad K, Ytrehus B, Ekman S, et al. 2008. Epiphyseal cartilage canal blood supply to the distal femur of foals. Equine Vet J 40:433-439.

25. Olstad K, Ytrehus B, Ekman S, et al. 2008. Epiphyseal cartilage canal blood supply to the tarsus of foals and relationship to osteochondrosis. Equine Vet J 40:30-39.

26. Olstad K, Ytrehus B, Ekman S, et al. 2009. Epiphyseal cartilage canal blood supply to the metatarsophalangeal joint of foals. Equine Vet J 41:865-871.

27. Ytrehus B, Carlson CS, Lundeheim N, et al. 2004. Vascularisation and osteochondrosis of the epiphyseal growth cartilage of the distal femur in pigs-- development with age, growth rate, weight and joint shape. Bone 34:454-465.

28.   Carlson CS, Hilley HD, Meuten DJ. 1989. Degeneration of cartilage canal vessels associated with lesions of osteochondrosis in swine. Vet Pathol 26:47-54.

29.   Olstad K, Ytrehus B, Ekman S, et al. 2007. Early lesions of osteochondrosis in the distal tibia of foals. J Orthop Res 25:1094-1105.

30.   Olstad K, Ytrehus B, Ekman S, et al. 2011. Early lesions of articular osteochondrosis in the distal femur of foals. Vet Pathol 48:1165-1175.

31.   Woodard JC, Becker HN, Poulos PW. 1987. Articular cartilage blood vessels in swine osteochondrosis. Vet Pathol 24:118-123.

32.   Ytrehus B, Ekman S, Carlson CS, et al. 2004. Focal changes in blood supply during normal epiphyseal growth are central in the pathogenesis of osteochondrosis in pigs. Bone 35:1294-1306.

33.   Pfeifer CG, Kinsella SD, Milby AH, et al. 2015. Development of a Large Animal Model of Osteochondritis Dissecans of the Knee: A Pilot Study. Orthop J Sports Med 3:2325967115570019.

34.   Carlson CS, Meuten DJ, Richardson DC. 1991. Ischemic necrosis of cartilage in spontaneous and experimental lesions of osteochondrosis. J Orthop Res 9:317-329.

35.   Ytrehus B, Andreas Haga H, Mellum CN, et al. 2004. Experimental ischemia of porcine growth cartilage produces lesions of osteochondrosis. J Orthop Res 22:1201-1209.

36. Olstad K, Hendrickson EH, Carlson CS, et al. 2013. Transection of vessels in epiphyseal cartilage canals leads to osteochondrosis and osteochondrosis dissecans in the femoro-patellar joint of foals; a potential model of juvenile osteochondritis dissecans. Osteoarthritis Cartilage 21:730-738.

37. Toth F, Torrison JL, Harper L, et al. 2016. Osteochondrosis prevalence and severity at 12 and 24 weeks of age in commercial pigs with and without organic-complexed trace mineral supplementation. J Anim Sci 94:3817-3825.

38. Van Grevenhof EM, Ducro BJ, Van Weeren PR, et al. 2009. Prevalence of various radiographic manifestations of osteochondrosis and their correlations between and within joints in Dutch warmblood horses. Equine Vet J 41:11-16.

Figures

Figure 1: Three-dimensional reconstructions of the quantitative susceptibility maps depicting the vascular architecture of the distal femoral epiphyseal cartilage in the transverse (axial) plane in miniature pigs (18, 33, and 48 days old) and a human being (4 months old) (see also supplementary video material). Note the presence of distinct axial (central) and abaxial (peripheral) vascular beds both in the miniature pigs and in the human subject with vessels oriented parallel to the articular surface creating a characteristic avascular region (white arrows) in the midsagittal plane. All specimens are oriented with the medial aspect towards the left and the anterior (cranial) aspect towards the top of the figure.
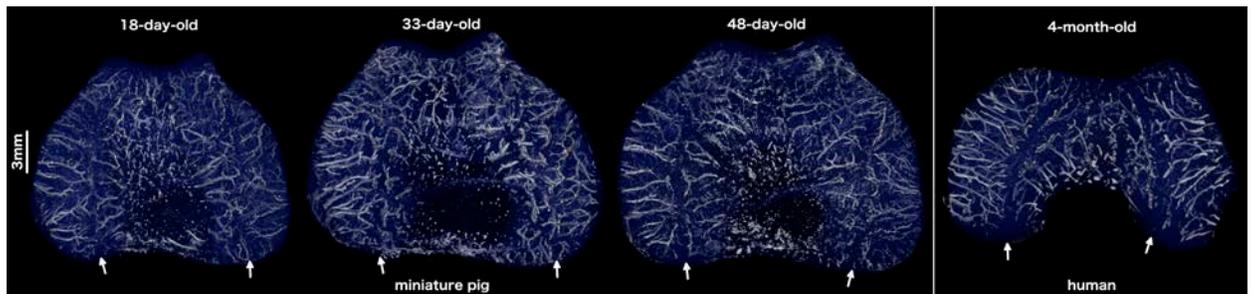

Figure 2: T2-weighted MRI of the left distal femur of miniature pig 2 (panel A) obtained 64 days after surgical interruption of the epiphyseal vascular supply to the abaxial aspect of the medial femoral condyle. The white circle marks an area of T2 hyperintensity consistent with epiphyseal cartilage necrosis within the medial femoral condyle. Photomicrograph (Panel B) depicts a coronal section through the medial femoral condyle. Black dashed line marks a discrete area of epiphyseal cartilage necrosis (OC-latens). Degenerate vessels within the area of epiphyseal cartilage necrosis are marked by black arrowheads. Area identified by the black rectangle is depicted in panel C at ten-times

higher magnification. In panel C, a black asterisk marks an area of cystic matrix degeneration (an area where loss of tissue/matrix components results in clear spaces replacing the matrix) within an island of necrotic epiphyseal cartilage. Arrows indicate chondrocyte clones along the margin of the area of necrosis. Hematoxylin and eosin stain.
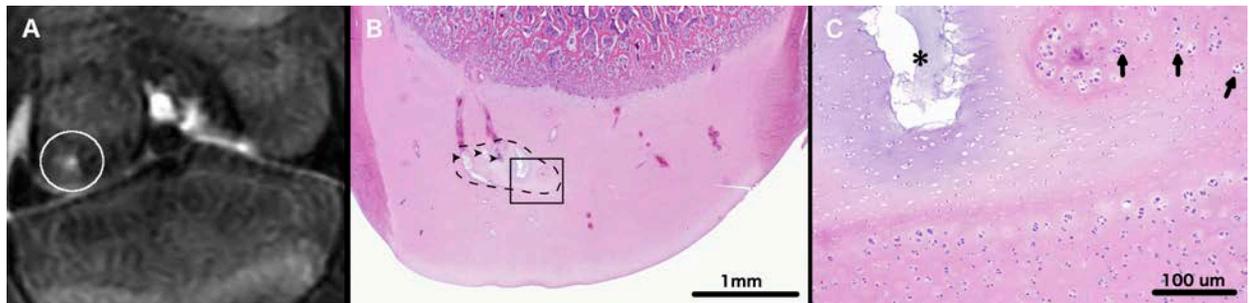

Figure 3: T2-weighted MRI of the left distal femur of miniature pig 1 obtained 18 (panel A), 28 (panel B) and 63 days (Panel C) after surgical interruption of the epiphyseal vascular supply to the abaxial aspect of the medial femoral condyle. White circles mark areas of T2 hyperintensity consistent with epiphyseal cartilage necrosis (panels A to C). Photomicrograph (Panel D) depicting a coronal section through the medial femoral condyle showing an area of epiphyseal cartilage necrosis (dashed line), and associated delay in enchondral ossification (OC manifesta), corresponding with the lesion identified by the white circle in Panel C. Black asterisk marks an area of revascularization within necrotic epiphyseal cartilage. Panel E shows the area indicated by the black rectangle in panel D at twenty times higher magnification. In panel E chondrocyte clones are present at the interface (dashed line) of necrotic (upper half of image) and viable (lower half of image) epiphyseal cartilage. Hematoxylin and eosin stain.
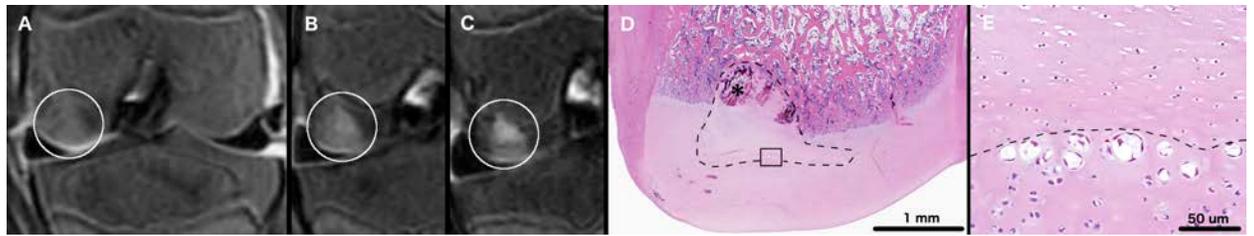
Figure 4: T2-weighted MRI of the left distal femur of miniature pig 3 (panel A) obtained
63 days after surgical interruption of the epiphyseal vascular supply to the abaxial aspect
of the medial femoral condyle. A white circle marks an area of T2 hyperintensity
consistent with epiphyseal cartilage necrosis. Photomicrograph (Panel B) depicting a
coronal section of the medial femoral condyle with a dashed line marking an area of
epiphyseal cartilage necrosis and focal failure of enchondral ossification (OC manifesta),
corresponding with the lesion identified by the white circle in Panel A. Areas marked by
indicate trapped stain (artifact). The area outlined by the black rectangle is depicted in
panel C at ten-times higher magnification. Arrows mark chondrocyte clones present
along the margins of the area of epiphyseal cartilage necrosis. Asterisk is centered on a
discrete area of cartilage necrosis characterized by pallor of the extracellular matrix and
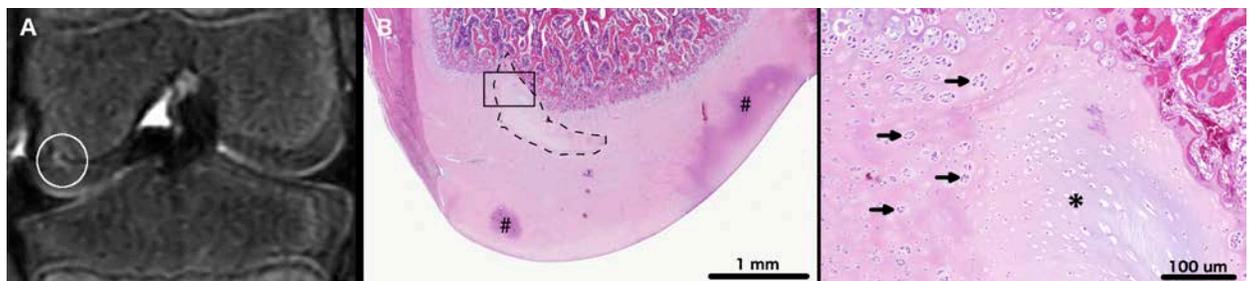necrotic chondrocytes. Hematoxylin and eosin stain.

Table 1: Results of three consecutive MRI examinations of 4 miniature pigs after surgical interruption of the vascular supply to the axial or abaxial aspect of the medial femoral condyle.

	MFC operated	MRI Scan 1 (time of scan [day])	MRI Scan 2 (time of scan [day])	MRI Scan 3 (time of scan [day])
Pig 1	right - axial	NSF (18)	NSF (28)	NSF* (63)
	Left - abaxial	T2 hyperintensity OC latens (18)	T2 hyperintensity OC latens (28)	T2 hyperintensity OC manifesta* (63)
Pig 2	right - axial	NSF (18)	NSF (30)	NSF* (64)
	Left - abaxial	NSF (18)	T2 hyperintensity OC latens (30)	T2 hyperintensity OC latens* (64)
Pig 3	right - axial	NSF (19)	NSF (32)	NSF* (63)
	Left - abaxial	NSF (19)	NSF (32)	T2 hyperintensity OC manifesta* (63)
Pig 4	right - axial	NSF (19)	NSF (40)	NSF* (69)
	Left - abaxial	NSF (19)	NSF (40)	NSF* (69)

NSF: No significant finding

*: Lesions that were confirmed histologically